# RSC Advances

# Journal Name

Dynamic Article Links ▶

# ARTICLE TYPE

# Energy-saving and environmentally friendly electrodeposition of γ-MnO₂

## Jing Tang,  Hui-Min Meng*, and Liang Liang Hang

The paper reports a new energy-saving and environmentally friendly method for synthesis of γ-MnO₂ using a Pt/C gas diffusion electrode instead of the traditional cathode. The Pt/C gas diffusion electrode has high activity in a $120g \cdot dm^{-3}$ $MnSO_4 \cdot H_2O + 30g \cdot dm^{-3}$ $H_2SO_4$ electrolyte at 80℃. At the same time, the cell voltage and electrode potential of electrolytic cell with Pt/C gas diffusion electrode as cathode are measured at $100A \cdot m^{-2}$ for 12h. The results show that the Pt/C gas diffusion electrode demonstrated good stability. The
10 effects of the current density on the synthesis of γ-MnO₂ (EMD) is studied, and the results show that the electric energy consumption of the GDE as cathode drops 61.06%-57.75%,65.6%-62.9% and 61.4%-55% compared with that of the Cu, Graphite, Pt cathode at $80A \cdot m^{-2}$, $100A \cdot m^{-2}$, $120A \cdot m^{-2}$ respectively in 12 hours. The γ-MnO₂ (EMD) shows a better discharge performance as cathode material of Zn-MnO₂ than the commercial battery grade manganese dioxide.
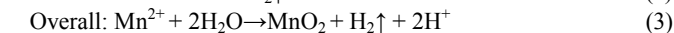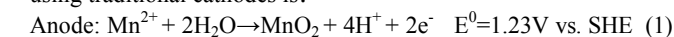
## Introduction

15 Energy and environment are among the most important issues in the twenty-first century[1]. The batteries which are used as green energy have caused wide public concern. The γ-MnO₂, which is an environmentally friendly, safe, a low cost material and relatively high discharge voltage compared to the α-, β-, and δ-
20 MnO₂[2] has been reported to be as cathode active material[3,4] in batteries.

　　The γ-MnO₂ used in batteries can be categorized as three groups: natural manganese dioxide (NMD), chemical manganese dioxide (CMD) and electrolytic manganese dioxide (EMD),
25 according to the production method[5]. The CMD is synthesized by chemical method (oxidation method). The synthesis process of γ-MnO₂ (EMD) is that the cathodes and anode are placed in an aqueous bath of $MnSO_4$ and $H_2SO_4$ solution with a constant current under atmospheric conditions and then the high purity and
30 high density γ-MnO₂ (EMD) is directly deposited on the anode surface. The electrodeposition process of γ-MnO₂ has better control over the properties of the deposited material than the chemical synthesis[6] and higher yield densities of γ-MnO₂ (EMD), comparing with that of γ-MnO₂ (CMD)[7]. Hill[8] found that γ-MnO₂
35 (EMD) materials are higher in energy than γ-MnO₂ (CMD) variants, and this is because the γ-MnO₂ (EMD) is characterized by the larger proportion of ramsdellite and microtwinning. In recent years, the nano γ-MnO₂ (coprecipitation[9], reflux[10] and hydrothermal synthesis[11]) used in supercapacitor[12], battery[13] and
40 catalyst[14] has been synthesized. But the γ-MnO₂ (EMD) has a much lower price comparing nano γ-MnO₂. As a result EMD (electrolytic γ-manganese dioxide) has become the most widely used materials in battery, such as alkaline[15] and lithium cells[16].
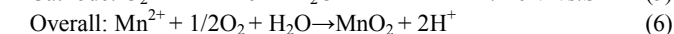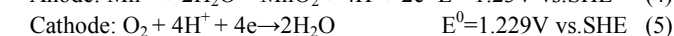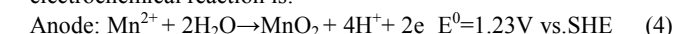
　　With increasing electrically powered consumer products, the
45 demand for γ-MnO₂ is also ever-growing. The γ-MnO₂ (EMD) demand is more than 349,000 mt in 2011 and grows at a 5.3% CAGR from 2011 to 2016. Enormous research has been done

50 about γ-MnO₂ (EMD). For example, Ghaemi et al[17]. have reported the electrodeposition of manganese dioxide in acidic $MnSO_4$ solution and the cell voltage usually floated between 2.3 V and 2.4V using graphite as cathode. Biswal et al[18]. have reported energy consumption of EMD at $100A/m^2$ was 1660
55 KWh/t. But the synthesis of γ-MnO₂ (EMD) is a very energy demanding and large volumes of hydrogen gas is generated at the cathode. However, the hydrogen gas carries acidic mist into the air, of which some spreads throughout the workplace. Not only is this acidic mist hazardous to health but also it damage the
60 environment[19]. It is necessary, therefore, to reduce the energy consumption and hydrogen gas emission in view of the issue of environmental pollution. Replacing the traditional cathode with a Pt/C gas diffusion electrode (GDE) significantly reduces the cell voltage, because of the potential difference between the oxygen
65 reduction reaction of Pt/C GDE and the hydrogen evolution reaction of the traditional cathode (Cu, Graphite, Pt). It is well known that electrodeposition reaction of manganese dioxide using traditional cathodes is：

Anode: $Mn^{2+} + 2H_2O \rightarrow MnO_2 + 4H^+ + 2e^-$  $E^0$=1.23V vs. SHE  (1)
70 Cathode: $2H^+ + 2e^- \rightarrow H_2\uparrow$　　　　$E^0$=0V vs. SHE  　(2)
Overall: $Mn^{2+} + 2H_2O \rightarrow MnO_2 + H_2\uparrow + 2H^+$　　　(3)
Where $E^0$ is the electrode potential vs.SHE. The decomposition voltage $E^0$ of the total electrode reactions is 1.23V.

　　If a gas diffusion electrode is employed in the electrolytic
75 manganese dioxide cell instead of the traditional electrode, the electrochemical reaction is:

Anode: $Mn^{2+} + 2H_2O \rightarrow MnO_2 + 4H^+ + 2e$  $E^0$=1.23V vs.SHE  　(4)
Cathode: $O_2 + 4H^+ + 4e \rightarrow 2H_2O$　　　　$E^0$=1.229V vs.SHE  (5)
Overall: $Mn^{2+} + 1/2O_2 + H_2O \rightarrow MnO_2 + 2H^+$　　　(6)
80 　　The decomposition voltage $E^0$ of the total electrode reactions is 0.001V. The decomposition voltage drops by 1.229V comparing to the traditional cathode. Fig.1 shows the schematic diagrams of electrolysis with the Pt/C GDE. It is anticipated that the use of a
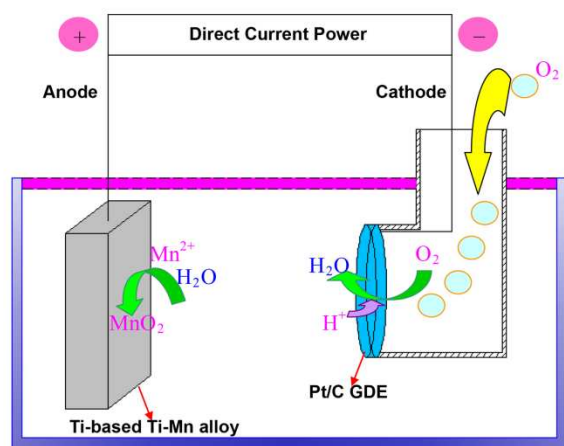
RSC Advances Accepted Manuscript

**Fig.1** The schematic diagrams of the Pt/C GDE electrolysis



**Fig.3** CV of the GDE in a 120g·dm-3 $MnSO_4·H_2O+30g·dm^{-3}$ $H_2SO_4$ electrolyte at 80℃, Scan rate: 20 mV $s^{-1}$ in air at the flow rate of 30ml/min

5 Pt/C GDE can save the energy of 90% under standard conditions. Therefore, not only can energy savings be obtained through the introduction of the Pt/C GDE, but also this method protects environment.

With this context, we study the possibility of utilizing a Pt/C 10 GDE as cathode in electrolysis process. The energy-saving mechanism of the Pt/C GDE is discussed using cyclic voltammetry (CV). The energy consumption of electrolysis bath with the Pt/C GDE is compared to the Cu, Graphite, Pt cathode by electrolytic experiments. The discharge characteristic of γ-15 $MnO_2$ (EMD) is tested.

## Results and discussion

Fig. 2A exhibits XRD patterns of the Pt/C samples. The first broad peak located at 25° which was associated with the Vulcan XC-72R support material. The Pt peaks appeared at 39.76°, 20 46.24°, 67.46°and 81.28°, which were attributed to the (111), (200), (220), and (311) planes of face-centered cubic structure[20,21] of Pt (JCPDS PDF#70-2057), respectively. The macroscopic properties of Pt/C such as surface morphology, particle size, and metal dispersion were investigated by TEM. TEM micrographs of 25 40wt% Pt/C are shown in Fig. 2B. It is observed that the Pt
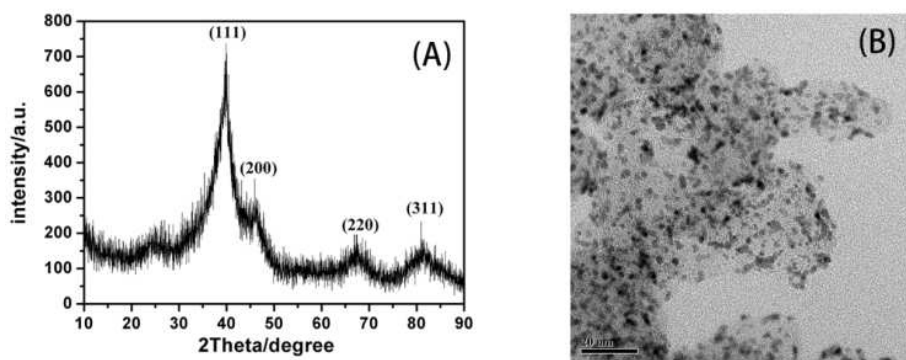
30 particles were well dispersed on the carbon support and most of the particles were in the range of 2-3 nm. Fig. 3 shows CV of the Pt/C GDE surface at air. It is clearly seen that the reduction peak is at 0.6V - -0.05 vs. Hg/HgSO4 and the high reduction peak is at 35 about 0.1V vs. Hg/HgSO4, According to redox potential, this reduction current peaks can be attributed to the formation of $O_2$ to $H_2O$. The current density increased linearly from 0.6V to 0.1V using Pt/C GDE in electrolyte at air indicating that the Pt/C GDE has high activity[22]. The window voltage of ORR was so big, 40 which could be attributed to the intrinsic properties of the gas diffusion electrode. The electrode/electrolyte/gas three-phase boundaries of GDE have higher solubility of oxygen in electrolyte[23].

The cell voltage, cathode potential and anode potential time 45 curves of electrolysis with Pt/C GDE and Cu cathode were measured at the same time, at 100A·m⁻² for 12h. As shown in fig. 4A, the cathode potential versus Hg/HgSO4 of the gas diffusion electrode slightly vibrated with time and range of the voltage fluctuation was only ±0.007V, suggesting that the Pt/C GDE was 50 almost steady. The average cathode potential of gas diffusion electrode was -0.02V versus Hg/HgSO4 at 100A·m⁻². However, the average cathode potential of Cu electrolysis was as high as -1.10 V. This indicates that the cell voltage could reduce from -1.10 V to -0.02 V due to the potential of oxygen reduction
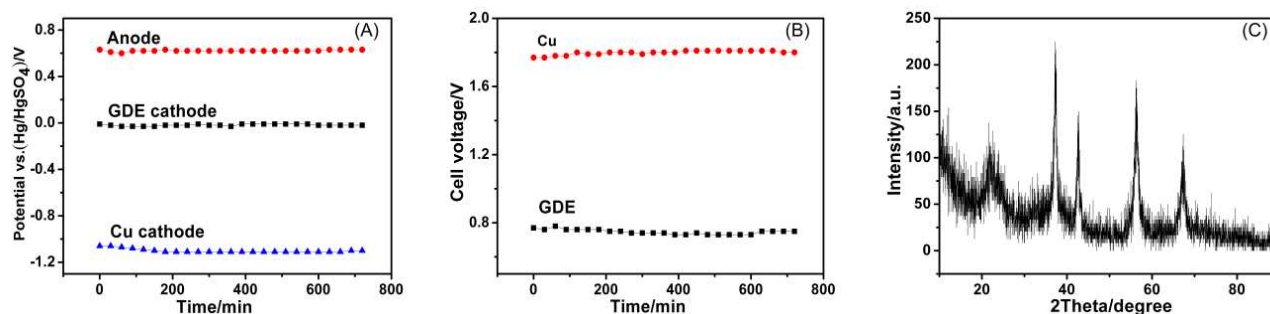
55



**Fig.2** XRD patterns (A) and TEM image (B) of 40wt% Pt/C catalysts

**Fig. 4** Electrolytic experiments of the GDE cathode and Cu cathode: (A): electrode potential (B) cell voltage (C) the product of electrolysis

**Table. 1** The effect of the current density on electrolytic

| Current density | Cathode | Average cathode Potential (V vs. $Hg/HgSO_4$) | Average anode Potential (V vs. $Hg/HgSO_4$) | Average Potential (V) | Cell Energy consumption (KWh/t) |
|---|---|---|---|---|---|
| 80 A/m$^2$ | GDE | 0 | 0.601 | 0.70 | 437.8 |
| | Cu | -1.05 | 0.608 | 1.71 | 1124.2 |
| | graphite | -1.23 | 0.597 | 1.95 | 1271.2 |
| | Pt | -1.03 | 0.614 | 1.70 | 1133.3 |
| 100A/m$^2$ | GDE | -0.02 | 0.621 | 0.75 | 471.0 |
| | Cu | -1.10 | 0.614 | 1.80 | 1187.2 |
| | graphite | -1.32 | 0.627 | 2.02 | 1268.5 |
| | Pt | -1.10 | 0.650 | 1.80 | 1130.4 |
| 120A/m$^2$ | GDE | -0.03 | 0.659 | 0.81 | 516.6 |
| | Cu | -1.12 | 0.652 | 1.85 | 1222.8 |
| | graphite | -1.43 | 0.628 | 2.18 | 1391.7 |
| | Pt | -1.14 | 0.657 | 1.81 | 1148.3 |

is higher than that of hydrogen evolution[24,25]. The cell voltage drop (1.08V) is less than theoretical value(1.23V) which is due to overpotential of the oxygen reduction reaction[26]. Not all oxygen molecule is reduced to $H_2O$ (direct 4-electron route), and part of oxygen molecule may be reduced to $H_2O_2$[27,28] and then be reduced to $H_2O$.

Fig. 4B exhibits the cell voltages of the electrolysis bath with Pt/C GDE and Cu cathode corresponding to cathode potential with Pt/C GDE cathode and Cu cathode shown in Fig. 3A. The voltage kept fluctuation range within ±0.014mV and the average cell voltages of the electrolysis bath with Pt/C GDE was 0.748V. However, standard cell potential was 0.64V, and that is because the $iR_{cell}$ causes an increase in cell voltages as shown in Equation[29] (7).

$$E_{cell} = E_{anode} - E_{cathod} + \sum \eta + iR_{cell} \tag{7}$$

The average cell voltage of the electrolysis bath with Cu electrolysis was 1.798V, indicating that the cell voltage with Pt/C GDE decreased by 1.05V when compared with that of Cu cathode. Fig. 4C exhibits XRD patterns of the product of electrolysis. The first broad peak appeared at 22.3°and four sharper peaks appeared at 37.3°, 42.7°, 56.5°and 67.3° indicating that the product was γ-$MnO_2$. The result agrees with γ-$MnO_2$

models reported by Chabre and Parmetie[30].The batch electrolyses using Pt/C GDE as cathode and Cu $2 \times 2.5cm^2$ (Beijing Cuibolin Non-Ferrous Technology Developing Co., Ltd), Graphite $2 \times 2.5cm^2$ (Beijing Jixing Sheng an Industry & Trade Co., Ltd), Pt $2 \times 2.5cm^2$ (Beijing Cuibolin Non-Ferrous Technology Developing Co., Ltd) cathode as cathode were carried out to study the effects of the current density on the electrical energy consumption of electrolytic manganese dioxide. Table.1 displays the variation of electrical energy consumption and cell voltages with Pt/C GDE and Cu, Graphite, Pt cathode for same time (12h) at different current density. As expected, current efficiency decreased from 98.6% to 96.7% and the cell voltage of electrolysis with Pt/C GDE rose gradually from 0.70V to 0.81V with increasing the current density from 80 to 120A·m$^{-2}$. But the cell voltage of electrolysis with Pt/C GDE was lower than the cell voltage of electrolysis with Cu, Graphite, Pt cathode at same current density for same electrolysis time due to the low cathode potential of Pt/C GDE compared to the Cu, graphite, Pt cathode. The cell voltage of electrolysis with Pt/C GDE reduced less than 1.0V from 80 to 120A·m$^{-2}$ compared to the Cu, Graphite, Pt cathode. According to Pan et al[31]. the high cell voltage will cause a high
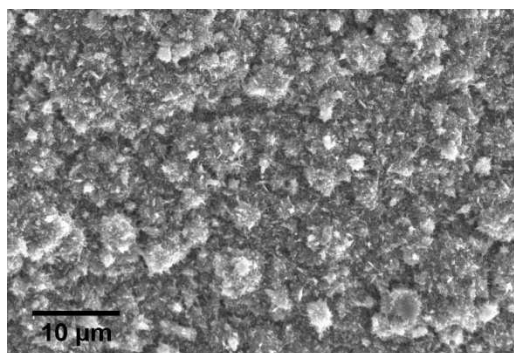
**Fig. 5** SEM image of γ-MnO$_2$(EMD) using Pt/C GDE as
5 cathode  at 80℃ in a 120g·dm$^{-3}$ MnSO$_4$·H$_2$O+30g·dm$^{-3}$ H$_2$SO$_4$ at
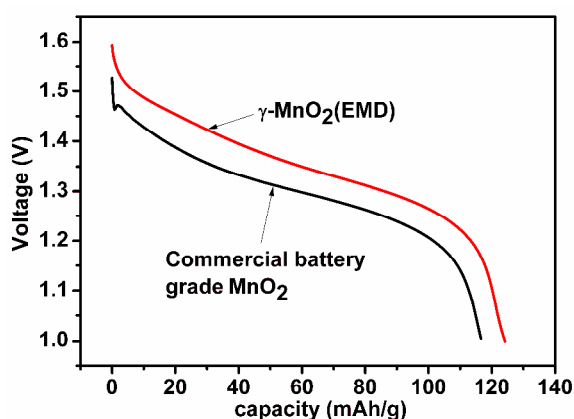100A·m$^{-2}$ for 12h



**Fig. 6** Discharge curves of γ-MnO$_2$(EMD) and commercial
10 battery grade MnO$_2$

energy consumption. Therefore, the electric energy consumption
of electrolysis with Pt/C GDE decreased due to a decrease in cell
voltage when compared with that of the Pt/C GDE. The decrease
15 in electric energy consumption of electrolysis with Pt/C GDE are
686.4-716.2 KWh/t and 833.4-875.1 KWh/t and 659.4-695.5
KWh/t, comparing with that of the Cu, Graphite, Pt cathode,
respectively at 80A·m$^{-2}$, 100A·m$^{-2}$and 120A·m$^{-2}$. It can be
concluded that electrolysis with Pt/C gas-diffusion cathode can
20 cut electric energy consumption by 61.06%-57.75%, 65.6%-
62.9% and 61.4%-55% compared to Cu, Graphite, Pt cathode at
80A·m$^{-2}$, 100A·m$^{-2}$ and 120A·m$^{-2}$ respectively in 12 hours.

The SEM image of the surface of ʏ -MnO$_2$(EMD) which was
deposited on the Ti-based Ti-Mn alloy anode and was obtained
25 by using Pt/C GDE as cathode  at 80℃ in a 120g·dm$^{-3}$
MnSO$_4$·H$_2$O+30g·dm$^{-3}$ H$_2$SO$_4$ at 100A·m$^{-2}$ for 12h is shown in
Fig. 5. It is clear that deposits which were piled on each other
were porous and irregular shapes. Fig. 6 compares the discharge
characteristics of EMD and commercial battery grade manganese
30 dioxide as cathodes in 9mol/L KOH electrolyte at the discharge
current density of 50mAg$^{-1}$ and the temperature of 25℃. The two
cells were discharged to a cut-off voltage of 1.0V. The open-
circuit potential of EMD was higher than the commercial battery

grade MnO$_2$. Note that the maximum discharge capacity γ-MnO$_2$
35 (EMD) is as high as 124.16mAh/g, which is higher than that of
commercial battery grade MnO$_2$, comparing with that of the
commercial battery grade manganese dioxide.

## Conclusions

The Pt/C GDE is successfully employed in the preparation of
40 electrolytic manganese dioxide in order to save energy and
protect the environment. The Pt/C GDE has high activity in
electrolyte and is almost steady. The electric energy consumption
of the electrolysis with Pt/C GDE can save 61.06%-57.75%,
65.6%-62.9% and 61.4%-55% comparing to Cu, Graphite, Pt
45 cathode at 80A m$^{-2}$, 100A m$^{-2}$ and 120A m$^{-2}$ respectively in 12
hours. The product of electrolysis is highly reactive γ-MnO$_2$. The
γ-MnO$_2$ (EMD) shows a better discharge performance as cathode
material of Zn-MnO$_2$ than the commercial battery grade
manganese dioxide. During the experiment process, there are no
50 releases of the toxic substance. Therefore, the electrolytic process
is high energy-saving and environmentally-friendly.

## Experiment

### Preparation of Pt/C gas diffusion electrode

55 The GDE consists of a three-layer structure which are diffusive
layer, substrate and catalyst layer. The diffusion layer was
prepared as follows: 295mg of acetylene black, 600mg of 60%
PTFE (Hesen, Shanghai, China), 307mg of Na$_2$SO$_4$, 300mg of
activated carbon powder, and 200mL of ethanol was used. The
60 above blend was mixed and stirred at 80℃ using magnetic
stirring apparatus and the resulting wet paste was rolled into a
0.4mm thin diffusion layer. The substrate was nickel screens. A
slurry for the catalyst layer was prepared by blending 50mg of
40% Pt/C (VXC72R) catalyst (Hesen, Shanghai, China), 200mL
65 of ethanol as a dispersant, 198mg of 60% PTFE (Hesen,
Shanghai, China), as a wet-proofing agent and binder, the 155mg
of acetylene black and 600mg of activated carbon powder. The
process of 0.3mm catalyst layer-making is same as the diffusion
layer. The Pt loading was 0.36±0.02 mg/cm$^2$. Catalyst layer and
70 diffusive layer were dried at 150℃ by electric drying oven in
order to remove surfactants of PTFE and then the diffusive layer
was rinsed in deionized water and dried in electric oven.
Furthermore, the diffusion layer was rolled on one side of the
nickel screens to give a flat sheet of 0.7mm thickness and then
75 the catalyst layer were pressed onto the other sides of nickel
screens to obtain about 0.8mm flat sheet.

### Electrolytic deposition process of γ-MnO$_2$

80 Electrolytic γ-MnO$_2$ experiments were carried out with three
electrodes at 80℃ in a 120g·dm$^{-3}$ MnSO$_4$·H$_2$O+30g·dm$^{-3}$ H$_2$SO$_4$
electrolyte in air, using a Ti-based Ti-Mn alloy as anode (Beijing
nonferrous metal research institute), a GDE as cathode and
Hg/HgSO$_4$ as reference electrode. The GDE was placed in a
85 PTFE holder and the gas flow passed over the diffusive layer of
the GDE cathode through a pipe inside the holder. The apparent
area of the GDE electrode face in contact with the solution was

5cm$^2$. A direct current power supply was employed to provide the direct current. During the electrolysis process the γ-MnO$_2$ is deposited directly on the anode immersed in the electrolysis cell, according to equation (1). At the end of this process of the electrolysis process, the electrolytic γ-MnO$_2$ is removed from the Ti-based Ti-Mn alloy anode. And then the electrolytic γ-MnO$_2$ was crushed, ground, repeatedly washed in water, neutralized by washing with 10% NaOH and repeatedly washed in water again until neutral and then dried in a drying oven. The electrolytic deposition process of γ-MnO$_2$ has the advantages of environment friendliness, simple operation and easy control.

### γ-MnO$_2$(EMD) discharge performance

The γ-MnO$_2$ (480mg) was first mixed with active carbon (120mg), acetylene black (60mg) and 60% PTFE (1000mg) as a binder and then mixture was pressed on nickel sheet. The discharged experiments were carried out with two electrodes at 25℃ in 9M KOH with the discharge current density of 50mAg$^{-1}$, using a mixture on a nickel sheet as working electrode and Zn sheet as counter electrode, using cs350 electrochemical work station.

### Characterization

X-ray diffraction analysis was carried out with a TTRⅢ X-ray power diffractometer using the Cu K_ (λ= 1.5405A˚) radiation source operating at 40 kV and 300 mA. The XRD patterns were measured in the range of 2θ=10°-90°scanning at the rate of 5°min$^{-1}$ with an angular resolution of 0.02°. The size and morphology distribution of Pt particles of catalyst were determined by TEM (JEM-2010F TEM microscope) using an accelerating voltage of 200 kV.

### Electrochemical measurement

The CV spectra were recorded using a CHI660 electrochemistry station with a standard a three-electrode consisting of a Ti-based Ti-Mn alloy electrode(16cm$^2$) as a counter electrode, an Hg/HgSO$_4$ as reference electrode, and the GDE as working electrode in air. During the experiment process, the temperature was kept at 80±2℃. The scan rate was 20mVs$^{-1}$.

### Acknowledgments

### Notes and references

*Beijing Corrosion and Protection Center, University of Science and Technology Beijing, No. 30, Xueyuan Road, Haidian District, Beijing 100083, China. Tel: +86 010 62332548; E-mail: menghm16@126.com*

1 Z. L. Wang, D. Xu, J. J. Xu , X. B. Zhang, *Chem. Soc. Rev.,* 2014.
2 W. I. Jung, M. Nagao, C. Pitteloud, K. Itoh, A. Yamada, R. Kanno, *J. Mater. Chem*, 2009, **19**, 800.
3 F. Y Cheng, J. Chen, X. L Gou, P. W. Shen, *Adv. Mater*, 2005, **17**, 2753.
4 S. Sarciaux, A. L. G. L. Salle, A. Verbaere, Y. Piffard, D. Guyomard, *J. Power Sources*. 1999, 81-82, 661.
5 T. X. T. Sayle, C. R. A. Catlow, R. R. Maphanga, P. E. Ngoepe, D. C. Sayle, *J. Crystal Growth*, 2006, **294**, 118.
6 K. R. Prasad, N. Miura, *J. Power Sources*, 2004, **135**, 354.
7 E. I. Wang, L. Lin, W. L. Bowden, US 5348726A, 1994.
8 J.R. Hilla, C. M. Freeman, M. H. Rossouw, *J Solid State Chem*, 2004, **177**, 165.
9 S.T Xing, R. R. Han, Z. C. Ma, Y. S. Wu, Z. C. Zhou. *CrystEngComm*, 2011, **13**, 6033.
10 X. Zhang, X. Z, Sun, H. T. Zhang, D.C. Zhang, Y.W. Ma. *Electrochim Acta*, 2013, 87, 637.
11 X.H Zhang, B.X. Li, C.Y. Liu, Q.X. Chu, F.Y. Liu, X.F. Wang, H.W. Chen, X.Y. Liu, *Mater Res Bull*, 2013, 48, 2696.
12 A. B. Yuan, X. L. Wang, Y. Q. Wang, J. Hu. *Energy Conver. Manage*, 2010, **51**, 2588.
13 F. Y. Tu, T. H. Wu, S. Q. Liu, G. H. Jin, C. Y. Pan, *Electrochimi Acta*, 2013, **106**, 406.
14 F. Y. Cheng , Y. Su , J. Liang , Z. L. Tao, J. Chen, *Chem. Mater,* 2010, **22**, 898.
15 C. Mondoloni, M. Laborde, J. Rioux, E. Andoni, C. Lévy-Clément, *J. Electrochem. Soc*, 1992, **139**, 954.
16 M. Manickam, P. Singh, T. B. Issa, S. Thurgate, R. D. Marco, *J. Power Sources*, 2004, **130**, 254.
17 M. Ghaemi, Z. Biglari, L. Binder, *J. Power Sources*, 2001, **102**, 29.
18 A. Biswal, B.C. Tripathy, K. Sanjay, M. K. Ghosh, T. Subbaiah, B. K. Mishra, *Hydrometallurgy*, 2011, **110**, 44.
19 R.A. Shakarji, Y.H. He, S. Gregory, *Hydrometallurgy*, 2013, **131-132**, 76.
20 L. Johnson, W. Thielemans, D. A. Walsh，*Green Chem*, 2011, **13**, 1686.
21 S. C. Zignani, E. Antolini, E. R. Gonzalez, *J. Power Sources*, 2008, **182**, 83.
22 L.J Li, A. Manthiram, *J. Mater. Chem. A*, 2013, **1**, 5121.
23 H. Cheng, K. Scott, *J. Electroanal. Chem*, 2006, **596**, 117-123.
24 Y. Tang, Y.J. Li, Y.Z. Sun, J.X. Wang, Y.M. Chen, X.J. Yang, P.Y Wan, *Green Chem*, 2012,**14**,334.
25 Y. Tang, Y.J. Li, Y.Z. Sun, J.X. Wang, Y.M. Chen, X.J. Yang, P.Y Wan, *Electrochem. Commun*, 2013, **27** 108.
26 I. E. L. Stephens, A.S. Bondarenko, U. Grønbjerg, J. Rossmeisl, I. Chorkendorff, *Energy Environ. Sci*, 2012, **5**, 6744.
27 M. Inaba, H. Yamada, J. Tokunaga, A. Tasaka, *Electrochem. Solid-State Lett*, 2004, **7**, A474.
28 A. Kishi, S. Shironita, M. Umeda, *J. Power Sources*, 2012, **197**, 88.
29 K. Zeng , D.K. Zhang, Prog. *Energy Combust. Sci*, 2010, **36**, 307.
30 Y. Chabre, J. Parmetier, *Prog in Solid State Ch*, 1995, **1**, 23.
31 J.Q. Pan, C. Zhang, Y.Z. Sun, Z.H. Wang, Y. S. Yang, *Chem. Commun*, 2012, **19**,70.